TAM Report No. 576

MICRO-PLASTIC STRAIN HYSTERESIS ENERGY AS A CRITERION FOR FATIGUE FRACTURE

by

C. E. Feltner and JoDean Morrow

Department of Theoretical and Applied Mechanics
University of Illinois
Urbana, Illinois

May, 1959

ABSTRACT

In this paper an energy criterion for fatigue failure is postulated. Micro-plastic strain hysteresis energy is considered to be the cause of fatigue damage. On this basis, a relation is developed between stress amplitude and the number of cycles to failure which utilizes only material properties obtained from the static true stress-strain tension test. The analysis is found to compare well with an experimentally determined S-N curve for soft SAE 4340.

ACKNOWLEDGMENT

This investigation was conducted in the Department of Theoretical and Applied Mechanics, as a part of the work of the Engineering Experiment Station of the University of Illinois. The subvention of Mr. C. E. Feltner through a University of Illinois graduate fellowship and the support of the Evendale Plant Laboratory of the General Electric Company under Contract Code Number 46 22 60 334 made this work possible.

Professor JoDean Morrow acted as project supervisor and Professor G. M. Sinclair contributed many helpful suggestions. Appreciation is due Mr. G. R. Halford who carried out the majority of the experimental tests. Mr. R. L. Moline helped in the reduction of data and preparation of figures. The manuscript was typed by Mrs. Nancy Dahl and Mrs. Anna Feltner.

TABLE OF CONTENTS

Page

LIST OF TABLES

LIST OF FIGURES

I. INTRODUCTION

When the problem of fatigue fracture was first studied nearly 100 years ago, investigators approached the problem by considering both stress and deformation. It was soon learned that a plot of alternating stress versus the logarithm of the number of cycles to fracture was approaximately a straight line. Stress, alone, furnished a convenient design criterion and was easy to control in laboratory tests. Fewer and fewer measurements of cyclic deformation were made, until about 1930 when nearly all effort in this direction ceased.

Efforts to understand the "fundamentals" of fatigue have been mostly centered around microscopic examination of slip bands and micro-cracks. Dislocation theory was introduced and now direct observations of dislocation formation and movement can be made. Such studies have helped to give a better qualitative concept of why metals are weak in fatigue.

Design is still, for the most part, based on a stress criterion. Allowable stresses are still obtained by running S-N curves for the material to be used under the conditions it is expected to experience in service.

In the last ten years, there has been a deviation from the stress criterion in the field of low cycle fatigue. For high stresses or strains resulting in fatigue lives of less than 10,000 cycles it has been found that the cyclic plastic strain range or the width of the hysteresis loop is a much more satisfactory quantity to correlate with fatigue life than is the stress. Further, it has been shown that the manner in which the cyclic plastic strain per cycle correlates with the fatigue

life depends on the static stress-strain properties of the material being tested.

Hence, the importance of measuring strain as well as stress has worked its way back into the philosophy of fatigue research. And why shouldn't it? The area under a stress-plastic strain curve is the amount of hysteresis energy converted during a fatigue cycle. This quantity is probably a more satisfactory criterion for fatigue damage than either stress or strain.

A. The Problem

If a cyclically loaded material exhibited a perfectly linear elastic relation between stress and strain, that is if there is no deterioration of the elastic energy, the material would be resistant to fatigue fracture. Obviously, to start with a specimen in one piece and then after the application of a finite number of load cycles find it to be in two pieces, requires a conversion of energy. The energy necessary to cause fracture is collected in small amounts during the course of the cyclic loading and is observable in terms of strain hysteresis. Therefore, if fatigue fracture is an energy conversion process and strain hysteresis is a measure of this energy, then strain hysteresis is the necessary quantity to study. This approach is the theme used in this paper.

B. Previous Work

A few investigations concerning energy conversion and its relation to fatigue failure have been made. Hysteresis is intimately related to the field of material damping in which a

large amount of work has been done.[1*] Only those investigations directly related to the study of hysteresis energy and fatigue behavior will be mentioned here.

The first study of this type was reported by Inglis[2] who measured the total energy to fracture of fatigue specimens subjected to rotating bending stresses. A plot of his results is shown in Fig. 1. No attempt was made to correlate this data. In 1947, Hanstock[3] made a study of the total energy to fracture for an aluminum alloy in alternating torsion. He suggested the equation,

$$\sum_{o}^{N} \Delta E = C + DN$$

where ΔE is the energy converted per cycle, N is the number of cycles and C and D are constants. The constant C was defined as the quantity of energy causing fracture while D was considered to be an energy quantity which did not contribute to the fracture process. Further experimental efforts[4] have been made in an attempt to verify this equation but have met with little success.

Efforts by Pardue, Melchor, and Good[5] and Duce[6] have been made to measure the total energy to fracture, but an energy criterion for fatigue fracture was not postulated.

There are many different mechanisms responsible for energy conversion during cyclic loading which are sensitive to a number of variables. A study of these factors has been made in

---

* Numbers indicate references included in the bibliography.

a previous paper.[7]

C. Purpose

To study fatigue failure from an energy viewpoint requires a knowledge of the stress and plastic strain during a cyclic test. Very little has been done to measure the stress and plastic strain in the most important stress region from a fatigue viewpoint, that is at and just above the fatigue limit. Measurements in this region are difficult to make due to the small inelastic strains which are involved. The present paper represents a preliminary attempt to directly measure the micro-plastic strains which are present near the fatigue limit, with the intention of correlating the hysteresis energy with fatigue behavior.

D. Scope

The scope of this investigation covers the testing of eight SAE 4340 specimens in an axial fatigue machine under conditions of controlled stress. True stress-true strain information was obtained for the same material.

Information on the fatigue properties and cyclic stress-strain behavior for this steel is given. An analysis is presented which permits the prediction of the S-N curve obtained. The analysis is based on energy as a criterion for fatigue failure and only material properties obtained from static stress-strain data.

II. EXPERIMENTAL INVESTIGATION

The material used in this investigation was SAE 4340 aircraft quality steel. The chemical analysis, heat treatment and engineering stress-strain properties of the material are given in Table 1.

To experimentally investigate hysteresis energy and fatigue behavior required a two-fold program. The first was to obtain static true stress-true strain properties of the material and the second was to obtain cyclic stress-strain measurements during the course of a fatigue test.

A. Static Tests

The true stress-strain static tension curve for a material is a more absolute and genuine representation of the phenomenon of flow and fracture than is the usual engineering stress-strain curve.[8] For this reason true stress-strain data was obtained for the 4340 steel in a static tension test.

1. Specimens: Solid cylindrical tension specimens were machined to the geometrical configuration and critical dimensions shown in Fig. 2. The l/d ratio for this specimen is 6.67. The specimens were lightly polished after heat treating and measurements of the test section were made to the nearest 0.0001-in. on a supermicrometer.

2. Apparatus: An Instron tension testing machine with a crosshead speed of 0.02-in. per minute was used to apply and measure the load from zero load to fracture. The accuracy to which the load could be read with the load cell on 5000 lbs. full scale was $\pm$10 lbs.

A modified version of a double ring diameter gage

as described by Pian and D'Amato[9] was used to measure the decrease in diameter of the specimen. The configuration of this gage is exhibited in Fig. 3. Four AD-7 wire resistance strain gages were attached as shown and electrically connected as an external four-arm bridge. This arrangement gives 400 percent increase in bridge output and provides temperature compensation.

Sensitivity of this gage was 36,300 microinches per inch of strain reading for a one inch change in opening of the contacts. Thus, 0.0001-in. change in opening of the contact gave a reading of almost 4 microinches which is approximately the accuracy to which the strain indicator used could be read.

A calibration curve was made before every test by means of a rod with step diameters from 0.0900-in. to 0.1600-in. in 0.0100-in. steps.

A micro-hardness tester with a 1.0 kg. load and a Knoop point was used to determine hardness measurements on small blocks of material which were heat treated with the specimens. Hardness values are given in Table 1.

3. Test Procedure: Specimens were fixed in the grips of the Instron machine with the diameter gage in place. The machine was calibrated and a zero diameter reading taken. The load was then applied and diameter readings were taken at approximately twenty-five intervals before fracture of the specimen. The final diameter measurement was made when the specimen was removed from the machine.

The test technique used consisted of setting a strain reading on the strain indicator and marking the load chart as the needle went by the null position. The Instron

machine is equipped with a button controlled device for marking the chart paper any time during the test.

B. Cyclic Tests

The monitoring of hysteresis loops during fatigue testing was performed by means of simultaneous stress and strain measurements. All tests were performed at a fixed amplitude of alternating stress about a zero mean stress.

1. Specimens: Thin walled tubular specimens were used for several reasons which are as follows: (1) they provide a small enough cross-sectional area so that their strength did not exceed the capacity of the machine used; (2) they provided a relatively large lateral surface area to which wire resistance strain gages could be attached; and (3) they reduce the possibility of buckling when axially loaded.

The geometry of the specimen and its dimensions are shown in Fig. 4. The specimens were cut to length and drilled through with a 5/16-in. gun drill. Next they were fitted to a mandrel and placed in a lathe where the threads and reduced section were machined. The specimens were then heat treated to the prescribed hardness. After being heat treated, they were honed on the inside, refitted to a mandrel, and finish polished on the outside. The inside surface was honed until there were no scratches visible to the naked eye and then was fine honed to a high polish.

The outside of the test section was mechanically polished with successively finer grades of emery cloth (grade Nos. 241, 1, and 00). By controlling the relative angular velocities between the polisher and the specimens and also the

translational speed and direction of the polisher, the fine scratches resulting from the final polishing were orientated nearly parallel to the axis of the specimen. In order to minimize residual stresses due to machining, the specimens were stress relief annealed in a vacuum at 900°F for one hour.

This machining and finishing process gave specimens which had an acceptable surface finish and concentricity of surfaces within 0.001-in.

2. Apparatus: The testing machine used was a modification of the one reported by Findley.[10] A schematic diagram of it is shown in Fig. 5. The machine is a constant amplitude of deflection type and has a capacity of approximately 3,000 lbs.

The present technique and method used for making extremely accurate stress-strain measurements does not allow high frequency measurements to be made. Since the normal operating frequency of the machine was 1200 cpm, it was necessary to install an auxiliary drive system for low frequency cycling. The frequency of operation with this system was 1/2 cpm and was slow enough to permit stress-strain measurements with a static strain indicator. It is known that frequency has an effect on the energy converted per cycle, however, for the range of frequencies used, this effect is small.[7]

3. Measuring Technique: Load was measured by use of a ring dynamometer employing four wire resistance strain gages. The gages were arranged in a four arm external bridge giving a 400 percent increase in bridge output and temperature compensation. The load cell was calibrated in a standard tension machine and had a calibration factor of 0.3897 lbs. per microinch/in.

Several methods of strain measurement were considered in the light of sensitivity and simplicity. Ultimately, four ABD-7 bakelite gages were attached to the specimen in the form of a four arm external bridge as shown in Fig. 6. This arrangement does not lend to simplicity since it requires a large supply of time, patience and bakelite strain gages. However, it does give remarkable sensitivity. The four arm external bridge with the two Poisson effect gages gives a 260 percent increase in bridge output and is the only method of attaining complete temperature compensation in an axially loaded specimen.

The average cross-sectional area of the specimens was 0.018 sq. inches. A one lb. change in load on an average specimen gave a reading of approximately 5 microinches in the elastic range. Sensitivity of this type is sufficient to provide quantitative results.

Due to the smooth surface finish on the specimens, nitro-cellulose bonded gages drifted. Bakelite gages were then used in an effort to achieve a better bond and more stability. Even with these, gage slip was encountered at the higher stresses and false negative permanent strains were observed.

A clip type extensometer with much lower sensitivity was then employed so that a constant check could be made on the strain gages on the specimen. It consisted of two heat treated steel loops with wire resistance strain gages mounted in the same manner as on the load cell. The loops were founded on the shoulders of the specimen to avoid fatigue failure at the gage point marks. In case the strain gages failed, the extensometer could be used for strain readings during the remainder

of the test. This served the purpose very well since an accurate calibration of the extensometer could be made during the early stages of a test. Also, this calibration compensated for any difference between strain measurements made from shoulder to shoulder over a gage length and those made directly on the test section.

4. Test Procedure: Bakelite strain gages were mounted on the specimen test section and were then subjected to a drying cycle, the maximum temperature reached being 250°F.

The specimen was placed in the machine free of initial stress with the aid of the distortion detector described in Ref. 10. The electrical circuit for the specimen strain gages was completed and the extensometer mounted in place.

With no load on the specimen, zero readings for the extensometer, load cell and specimen strain gages were recorded. The first few cycles were applied by hand while the eccentric was adjusted to insure completely reversed stressing. The slow frequency drive system could then be turned on and the machine allowed to slowly apply cyclic loading. The 1200 cpm drive system was operated intermittently until the specimen fractured, or the test was stopped. Measurements of stress-strain loops were made periodically throughout the test.

The procedure varied somewhat from one test to another. However, the method of taking readings was the same. The technique consisted of taking strain readings for the same loading and unloading values of stress. The method of analogous to the case where a specimen is dead weight loaded. As each weight is added a strain reading is taken until the maximum

desired stress is reached. Strain readings are again taken as each weight is removed, thus giving strain readings at the same stress level for the loading and unloading portions of the hysteresis loop. This is the principle by which the mechanical hysteresis loops were measured.

III. EXPERIMENTAL RESULTS AND DISCUSSION OF TRENDS

A. Results of Tests

1. Static Tests: The results of the static tension tests are given in Table 2 and Fig. 7 in the form of true stress-strain properties and the true stress-strain curve. Figure 7 was plotted by combining the data for the two specimens.

2. Cyclic Tests: Two types of information were obtained in this investigation: cyclic stress-strain data and fatigue data. The fatigue data is listed in Table 2. Figure 8 shows the results of the cyclic stress-strain measurements. Not only the maximum stress values, but all values of stress at which inelastic strains were measured are plotted in Fig. 8. This data was obtained early in the life ($N<3$ percent of the life to fracture) of six specimens. Values for tension and compression have been plotted together.

B. Discussion of Trends

1. Static Tests: In the region from the yield point to the ultimate load the true plastic strain is related to the true stress[11] by $\epsilon_p = k\sigma^{1/n}$. A plot of this equation on logarithmic coordinates is a straight line. The tension test data has been plotted in this manner and is shown in Fig. 9. The slope of this line, n, is known as the strain hardening exponent. The values of n obtained from the two specimens are listed in Table 2. The data for both specimens was combined and the slope computed by the method of least squares. The least squares value of the slope was $n = 0.0987$ which agrees closely with the average of the values taken from the two curves which is $n = 0.0985$.

2. Cyclic Tests: The data in Fig. 8 contains a large amount of scatter for two reasons which are: (1) it represents tension and compression data from six different specimens and (2) it is difficult to accurately measure such small quantities.

The line drawn through the data on Fig. 8 has a slope of one-half and appears to fit the data fairly well in the region of lower stresses. As the stress increases the data tends to fall to the right of this line.

Figure 10 shows a sample of the cyclic stress-strain behavior for a stress amplitude of 85 ksi. At a stress of this magnitude the hysteresis loop grows rapidly. Figure 11 gives the variation of hysteresis energy with the number of cycles and stress amplitude. The areas of the hysteresis loops, ΔW, for this plot were obtained by numerically integrating the cyclic stress-plastic strain data. The straight line on the semi-log plot shows the energy per cycle to be a growth process such that $\Delta W = Ce^{cN}$, where C is the ΔW value for $N = 0$, e is the base of natural logarithm and c is the slope of the lines on the semi-log plot of Fig. 11.

For specimens tested below $\pm$70 ksi., the change in the hysteresis loop was found to be small. The specimens tested below the fatigue limit showed either a constant value or a slight decrease of ΔW.

3. Interpretation of Static and Cyclic Stress-Strain Results: Figure 12 shows the relation between stress amplitude and total energy to fracture. The point (σ_f, U) from the static tension test has been plotted on this curve since it is the

minimum amount of energy that is required to fracture a specimen. A fatigue criterion based on constant energy to fracture would not be grossly in error except below the fatigue limit. If N goes to infinity at the fatigue limit the total energy converted must also go to infinity. Clearly, in order to introduce a fatigue limit, an analytical function for N in terms of energy must "blow up" to infinity at the fatigue limit. This could be introduced analytically, but it must be supported by a physical reason.

A clearer picture of the manner in which hysteresis energy is converted in a material can be obtained from a plot such as Fig. 13. The data for stresses near the fatigue limit (Fig. 8) and the static tension data (Figs. 7 and 9) are plotted on the same logarithmic plot.

In the region of low stresses the inelastic strain is largely composed of anelastic strain, since slip and plastic strain decrease rapidly as the stress decreases. The relationship between stress and anelastic strain for a ferromagnetic material may be expressed as,[7] $\sigma = k_z \epsilon_z^{1/2}$, where ϵ_z* is the anelastic strain. This relationship results from the fact that internal friction for a ferromagnetic material is linearly related to stress.[12] The line labeled "anelastic" in Fig. 13 has a slop of 1/2.

In the high stress region the ratio of the plastic strain to the anelastic strain is very large. Therefore, it is

---

* The z subscripts have been chosen from the first letter of C. Zener's name who did pioneering work in this field and coined the word "anelasticity."

a reasonable assumption to consider the inelastic strain in this region as entirely plastic.

Summing up, inelastic strain may be considered to be composed of anelastic strain and plastic strain. For high stresses the plastic strain dominates. For stresses below the fatigue limit the anelastic strain dominates. For stresses near the fatigue limit the two may be combined to form the curved portion of the solid line shown in Fig. 13.

By definition, fatigue damage does not occur below the fatigue limit where the inelastic strains are predominantly anelastic. Thus, anelastic strain energy is non-damaging from a fatigue viewpoint. The significant inelastic strain energy which causes fatigue failure must then be the plastic strain energy. If anelastic strain energy is considered to be non-damaging and plastic strain energy is considered to be damaging, a total energy to fracture versus stress amplitude curve similar to Figs. 1 and 12 would be obtained.

The slopes of the curves in Fig. 11 for stresses at or below the fatigue limit are slightly negative. This indicates an energy decay process. This energy decay is analogous to cyclic strain hardening and is probably related to it. Therefore, at stresses at or below the fatigue limit, the damaging plastic strain energy dies out before the minimum amount of total energy to cause fracture (U) is accumulated. Yet anelastic strain energy remains constant and is accumulated with each successive cycle. Thus, the total energy continues to increase. For high stresses the specimen fails when the total energy reaches a value just a little larger than the energy required

to fracture a static tension specimen.

In light of these observations, any analysis to establish an S-N curve using energy as a criterion for fatigue fracture should only include the plastic strain energy.

IV. ANALYSIS

Using the model of a stress-plastic strain hysteresis loop as shown in Fig. 14, it is possible to generate an S-N curve using only the static true stress-strain properties of the material. To do this, energy is used as the criterion for fatigue fracture.

A. Theoretical S-N Relationship*

For a reversed stress amplitude of σ_a the area under the σ-ϵ_p hysteresis loop for a single cycle, ΔW, may be written as,

$$(1) \quad \Delta W = dW/dN = 2\int_0^{\sigma_a} \sigma \, d\epsilon_p$$

where σ is some general stress level and ϵ_p is the plastic strain at that stress level.

In Fig. 11 it was shown that the energy per cycle changes with number of cycles for large stresses. However, note that for stresses in the region of ordinary fatigue (lives greater than 10^4 cycles) there is only a small change in the energy per cycle. Thus, it can be assumed with only a small error that the energy per cycle is only dependent on stress and is independent of duration of test.

The total energy converted by a specimen via damaging plastic strain hysteresis in N cycles, W_N, can be written as,

---

* The idea of this analysis was advanced by JoDean Morrow in "Speculative Remarks and Analysis Concerning Mechanical Hysteresis Energy as a Criterion for Fatigue Failure," a private communication to about 50 researchers in the field of flow and fracture, and the subject of a talk presented to members of the technical staff of the General Electric Company, Evendale, Ohio, March, 1959.

$$(2) \quad W_N = 2N\int_0^{\sigma_a} \sigma \, d\epsilon_p$$

The quantity W_N is assumed to increase until the capacity of the material to convert damaging energy in this fashion is exceeded at which time the body fails by fatigue. It can be assumed that the damaging energy to fracture in a fatigue test is constant and identical with energy to fracture in the static tension test, U, (see Fig. 12) the area under the static true stress-strain curve.

The only portion of the inelastic strain which is considered to cause fatigue damage is the plastic strain, ϵ_p, shown in Fig. 13. That due to the anelastic strain, also shown in Fig. 13, is considered to be non-damaging. It is impractical to measure ϵ_p at the stresses of interest because the anelastic strain ϵ_z, is the same order of magnitude as ϵ_p making it difficult to separate the two. For want of better measurements at stresses in the region of fatigue failure, the ϵ_p curve (Fig. 9) taken in the high stress region, where it is easily measured and is the dominating inelastic strain, can be extrapolated back to the low stresses of interest.

A logarithmic plot of σ and ϵ_p is linear as can be seen from Figs. 9 and 13. Thus,

$$(3) \quad \epsilon_p = \frac{\epsilon_c}{(\sigma_c)^{1/n}} (\sigma)^{1/n} = k(\sigma)^{1/n}$$

where σ_c and ϵ_c are any convenient corresponding values of true stress and true plastic strain taken in the region where plastic

strain dominates, and n is the slope of the curve in Fig. 9.

Differentiating Eq. (3) with respect to σ and substituting into Eq. (2) gives,

$$(4)\quad W_N = \frac{2kN}{n}\int_0^{\sigma_a} \sigma^{1/n} \cdot d\sigma$$

Integrating between 0 and σ_a gives,

$$(5)\quad W_N = \frac{2kN}{(1+n)}(\sigma_a)^{1+n/n}$$

At fracture $N = N_f$ and $W_N = U$. Substituting in Eq. (5) and rearranging terms leaves,

$$(6)\quad \frac{U(1+n)}{2k} = N_f(\sigma_a)^{1+n/n}$$

Taking the n/1+n root of both sides, and writing the equation in log form,

$$(7)\quad \log\left[\frac{U(1+n)}{2k}\right]^{n/n+1} - \left(\frac{n}{1+n}\right)\log N_f = \log \sigma_a$$

Using the symbol K for the first term in Eq. (7) which is constant for a specified material and set of test conditions, a simple equation for an S-N curve can be written,

$$(8)\quad \log \sigma_a = K - \left(\frac{n}{1+n}\right)\log N_f$$

This relationship which is based on a limiting constant plastic strain energy to fracture, plots as a straight line on a log σ_a vs. log N_f curve (see Fig. 15). The slope of the line is - n/1+n, and the intercept at one cycle (log N_f = 0)

is K.

B. Qualitative Comparison with Known Fatigue Behavior

One method of plotting usual fatigue data for lives between 10^4 and 10^7 cycles is a log σ_a - log N_f curve. The reason for this is that such a plot tends to make the data fall on a straight line such as Fig. 15. The slopes obtained for such plots are compatible with the theoretical value of the slope from Eq. (8) which is based on the slope of a static true stress-true plastic strain curve.

At least in ferrous materials the S-N plot shows a fatigue limit or a deviation from the straight line for low stresses such as shown by the dashed line to the right in Fig. 15. The analysis as presented in the preceding section does not predict such a fatigue limit.

For high stresses the logarithmic S-N_f plot also deviates from linearity as shown by the dashed line at the top of Fig. 15. The present analysis does not predict such a deviation. Since it is known that the hysteresis loop increases in area during the fatigue test at high stress amplitudes (see Fig. 11), then incorporating this fact in the analysis would produce a fatigue life curve at high stresses similar to the dashed line in Fig. 15.

C. Comparison of Experimental Results and Analysis

As pointed out in the preceding section, Eq. (8) does not apply in the high stress region or in the low stress region of fatigue (below the fatigue limit). In the intermediate range which is where most experimental S-N curves are established, Eq. (8) is reasonably valid.

Equation (8) was applied to the fatigue life data of this investigation and that of a previous investigation[13] on the same material. ONLY static stress-strain data is needed to apply Eq. (8). The static tension data for the two specimens reported in Table 2 were averaged for this purpose. These average values are: $U = 158{,}000$ lb-in/in^3, and $n = 0.0985$. For the values of σ_c and ϵ_c a convenient point on Fig. 9 was chosen. This point was $\sigma_c = 151{,}000$ psi. and $\epsilon_c = 0.08$ in/in.

Using these values the dotted line of Fig. 16 was constructed.

The agreement between the S-N curve established from the static stress-strain curve using energy as a criterion and the experimental points is extremely good except for the two portions of the curve which have been previously mentioned.

Most probably the close agreement is to some extent fortuitous, but by no means an accident. Preliminary attempts to extend the analysis to cover two harder sets of SAE 4340 fatigue data[13] did not meet with such good success. Equation (8) predicted longer lives than were measured, the worst agreement being for the hardest condition. It is believed that at least part of the difficulty stemmed from not having the proper static true stress-true strain data, and cyclic data such as reported in this paper. Static true stress-strain measurements may never replace experimental S-N curves, but at least this small amount of success offers some hope of reducing the number of cyclic tests required.

V. SUMMARY AND CONCLUSIONS

Hysteresis energy has been postulated as a criterion for fatigue failure. Specifically, the plastic strain energy portion of the hysteresis energy has been assumed to account for the damaging effects. Cyclic and static stress-strain studies have been conducted on SAE 4340 steel. An analytical relation between stress amplitude and fatigue life has been derived on the basis of four assumptions which are: (1) plastic strain energy is responsible for material damage; (2) a logarithmic plot of static true stress versus true plastic strain is valid when extrapolated back into the fatigue stress region; (3) the damaging energy per cycle for a given stress amplitude is the area under the static true stress-plastic strain curve depicted in Fig. 14; and (4) the total damaging energy required to cause fatigue fracture is constant and is equal to the area under the static true stress-true strain curve of Fig. 7.

The analysis is compared with the experimental results.

For the material listed in this investigation it may be concluded that: (1) hysteresis energy is a valid criterion for fatigue failure; (2) the static true stress-strain curve provides the necessary and sufficient information to predict fatigue life for stress amplitudes near and slightly above the fatigue limit; (3) cyclic stress-strain measurements serve to elucidate two facts which are: (a) the rapid growth of the hysteresis loop in the high fatigue stress region accounts for the erroneous prediction of longer lives than actually measured and (b) the slight decay of hysteresis energy for stresses at or below the fatigue limit demonstrates that damaging plastic strain hysteresis energy

dies out due to cyclic strain hardening before the critical energy to cause fracture (U) is accumulated.

The incorporation of the observations in parts (a) and (b) of the last paragraph into the analysis would tend to correct for the erroneously predicted long lives at high cyclic stresses and would introduce a fatigue limit.

VI. BIBLIOGRAPHY

1. Demer, L. J., "Bibliography of the Material Damping Field," WADC Technical Report 56-180, June, 1956.

2. Inglis, N. P., "Hysteresis and Fatigue of Wöhler Rotating Cantilever Specimen," The Metallurgist, pp. 23-27, February, 1927.

3. Hanstock, R. F., "Damping Capacity, Strain Hardening and Fatigue," Proc., Physical Society, Vol. 59, pp. 275-287, 1947.

4. Forrest, P. G. and Tapsell, H. J., "Some Experiments on the Alternating Stress Fatigue of a Mild Steel and an Aluminum Alloy at Elevated Temperatures," Proc. Inst. Mech. Engrs., Vol. 168, p. 763, 1954.

5. Pardue, T. E., Melchor, J. L., and Good, W. B., "Energy Losses and Fracture of Some Metals Resulting From a Small Number of Cycles of Strain," Soc. Exp. Stress Anal., Vol. VII, No. II, pp. 27-39, 1949.

6. Duce, A. G., "A Study of Some Fatigue Phenomena in Pure Metals and Alloys," Ph.D. Thesis, Univ. of Cambridge, England, 225 pp., 1950.

7. Feltner, C. E., "Strain Hysteresis, Energy, and Fatigue Fracture," TAM Report No. 146, Dept. of Theoretical and Applied Mechanics, Univ. of Illinois, June, 1959 (in press).

8. Feltner, C. E., "The True Stress-Strain Tension Test-Its Value To Engineering Research," Unpublished Research Report, Dept. of Theoretical and Applied Mechanics, Univ. of Illinois, March, 1959.

9. Pian, T. H. H. and D'Amato, R., "Low-Cycle Fatigue of Notched and Unnotched Specimens of 2024 Aluminum Alloy Under Axial Loading," WADC Technical Note 58-27, February, 1958.

10. Findley, W. N., "New Apparatus for Axial-Load Fatigue Testing," ASTM Bulletin No. 147, pp. 54-56, 1947.

11. Low, J. R. and Garofalo, F., "Precision Determination of Stress-Strain Curves in the Plastic Range," Soc. Exp. Stress Anal., Vol. IV, No. II, 1947.

12. Zener, C., Elasticity and Anelasticity of Metals, Univ. of Chicago Press, Chicago, Illinois, 1948.

13. Morrow, J. and Sinclair, G. M., "Cyclic Dependent Stress Relaxation," ASTM Symposium on Basic Mechanisms of Fatigue, STP No. 237, 1958.

TABLE 1

DESCRIPTION OF MATERIAL

Material: Aircraft Quality SAE 4340 Steel

Composition: C - 0.40, Mn - 0.81, P - 0.018, S - 0.019, Si - 0.25, Ni - 1.73, Cr - 0.87, Mo - 0.24

Heat Treatment: The fatigue, tension, and hardness specimens were austenitized at 1520°F in a neutral salt bath, quenched in still oil at room temperature and tempered at 1200°F for one hour. After the specimens were stress annealed one hour at 900°F.

Engineering Tensile Properties: Average tensile properties for two specimens are given in the table below. Knoop hardness of test blocks along with the approximate Rockwell C equivalent is also given.

Engineering 0.2% Offset Yield Strength, psi	Engineering Ultimate Strength, psi	Hardness Knoop 1 kg. load	Hardness Approx. Rockwell C
127,200	138,700	312	30.1

TABLE 2

SUMMARY OF TEST RESULTS

STATIC

Spec. No.	σ_f, psi	ϵ_f, in/in.	U, lb-in/in^3	n
S - 1	218,500	0.840	151,300	0.094
S - 1	228,200	0.895	164,500	0.103

CYCLIC

Spec. No.	$\pm \sigma_a$, psi	N_f	Total Energy to Fracture, W_f, lb-in/in^3
9	45,000	543,000(1)	287,000(1)
4	56,000	1,800,000(1)	1,850,000(1)
3	60,000	153,200	232,000
1	65,000(2)	257,800	576,000
12	72,200	67,100	no data
2	75,000	34,200	158,000
10	85,000	1,850	329,000
8	90,000	1,700	no data

(1) Did not fail - considered runout

(2) Tested for a few cycles at $\pm$35,000 psi

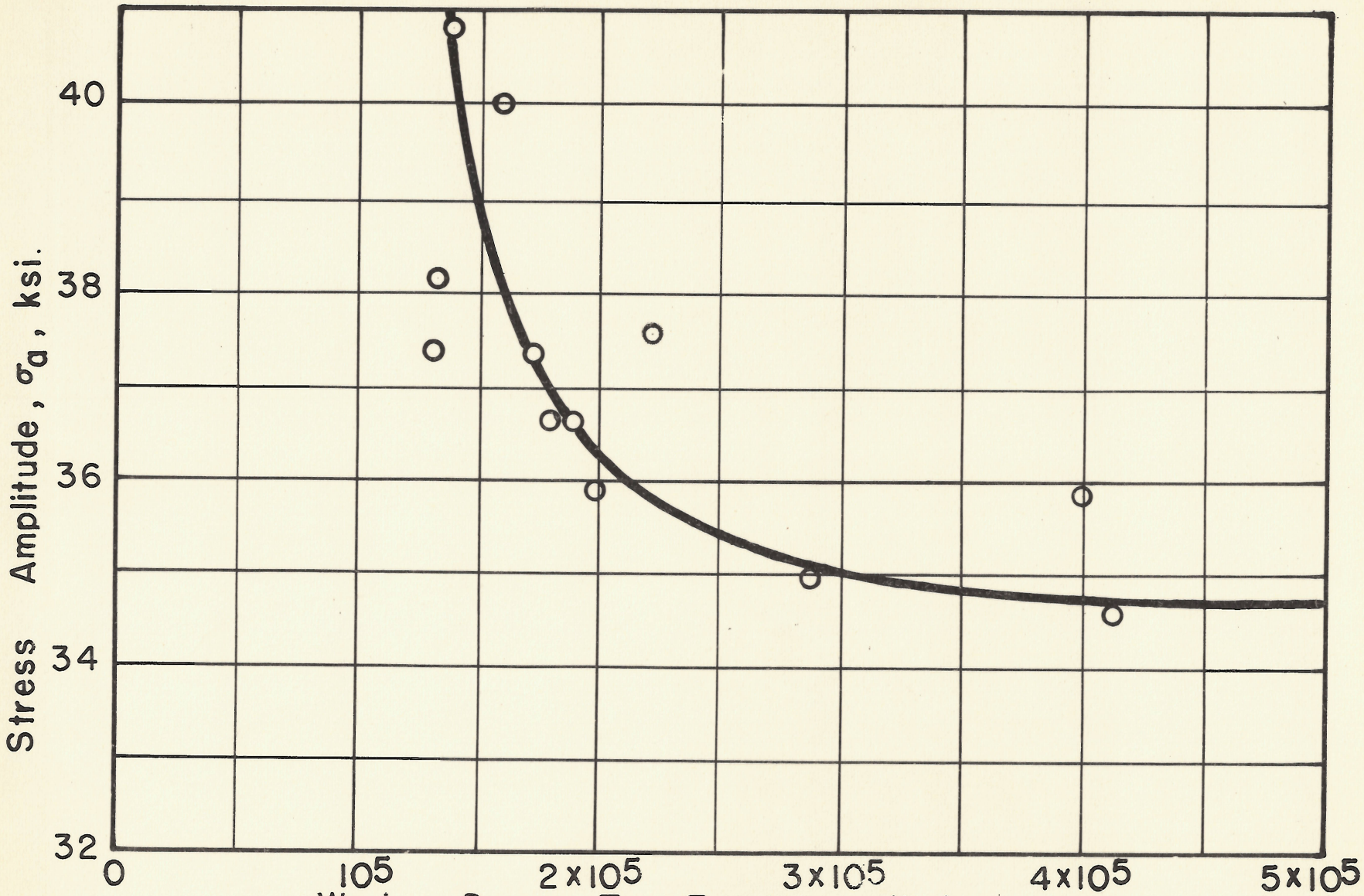

FIG. 1 - TOTAL WORK DONE TO FRACTURE FOR LOW CARBON STEEL (Ref. 2)

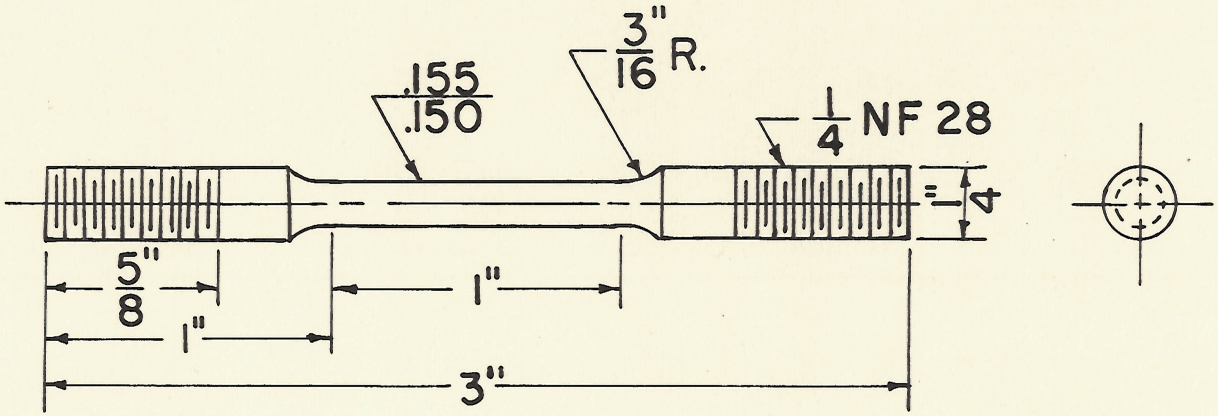

FIG. 2 - STATIC TENSION TEST SPECIMEN

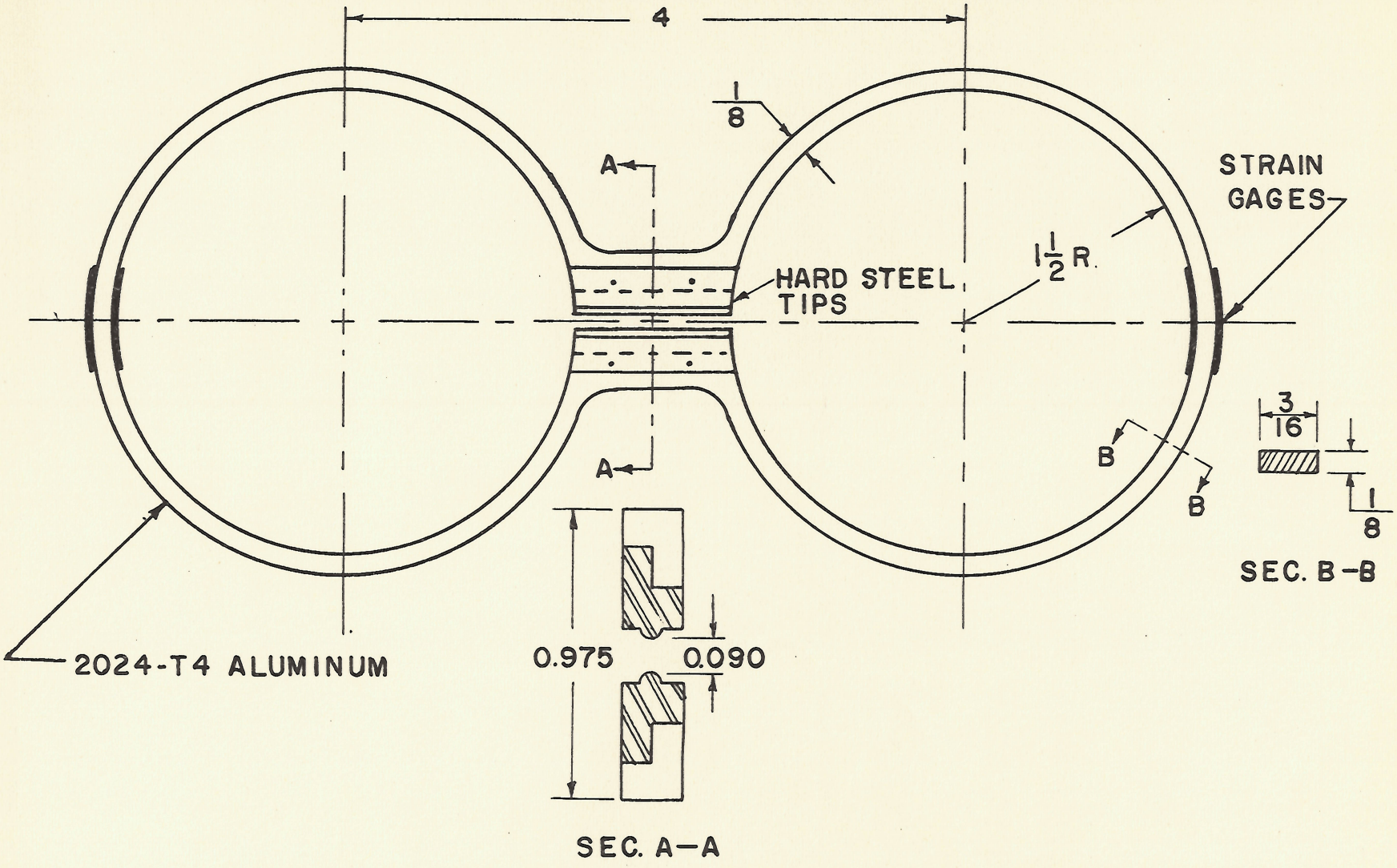

FIG. 3 - DOUBLE RING DIAMETER GAGE

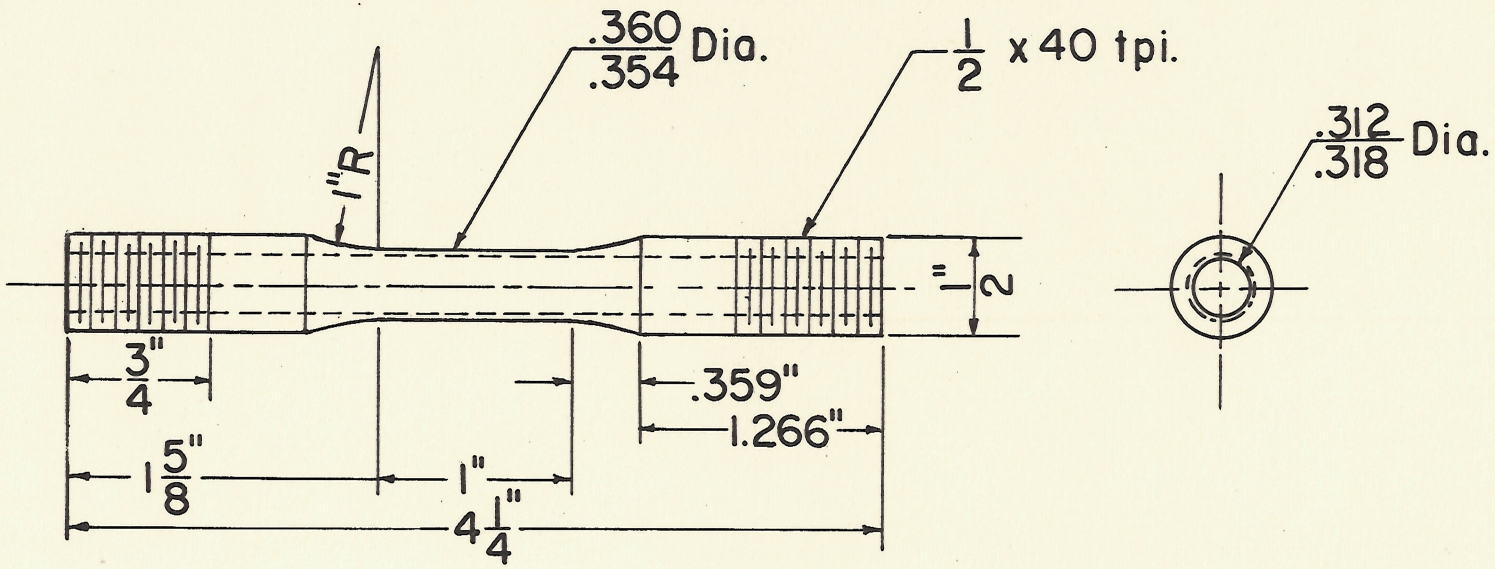

FIG. 4 - FATIGUE TEST SPECIMEN

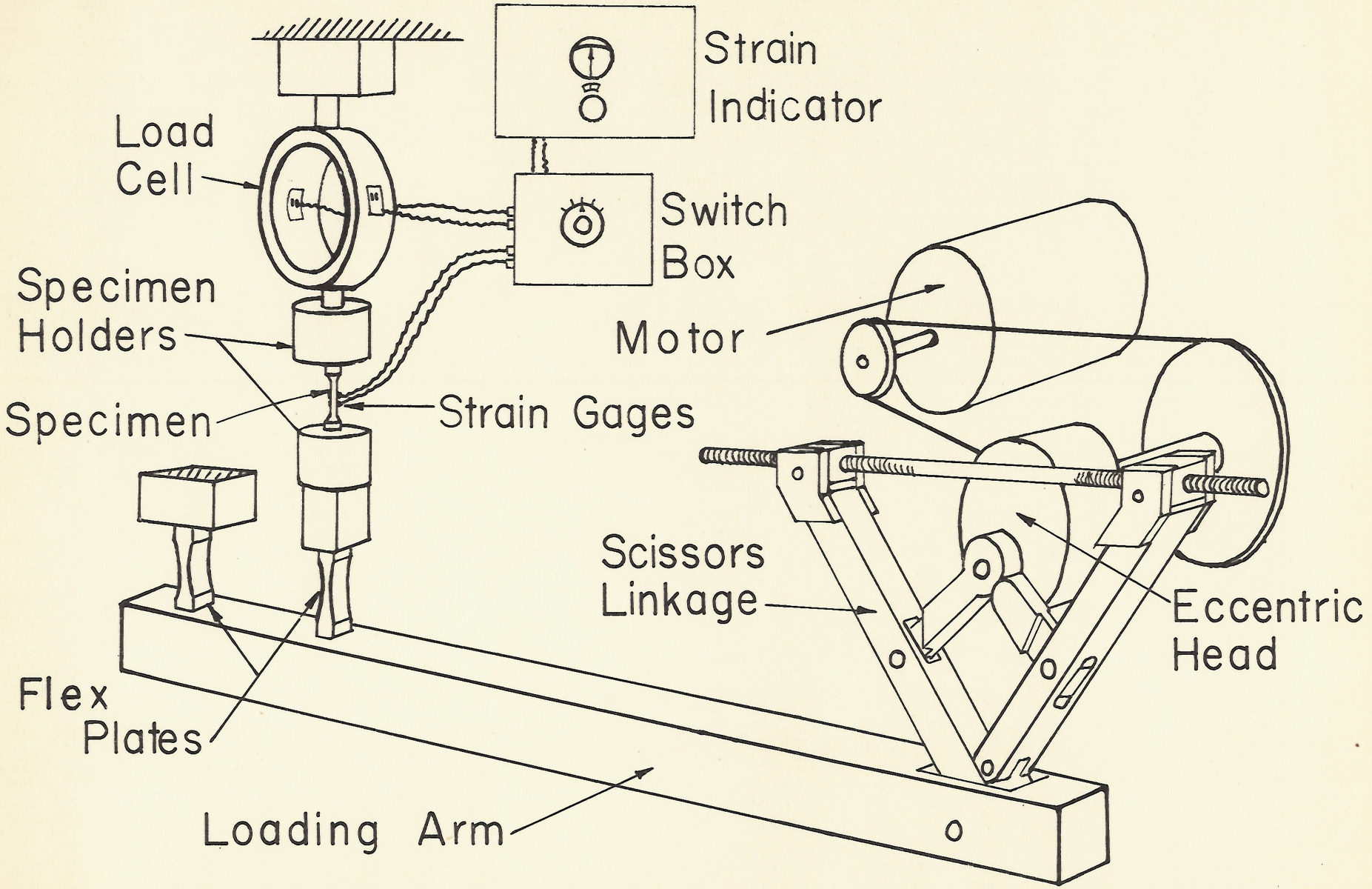

Fig. 5- Schematic Representation of Apparatus

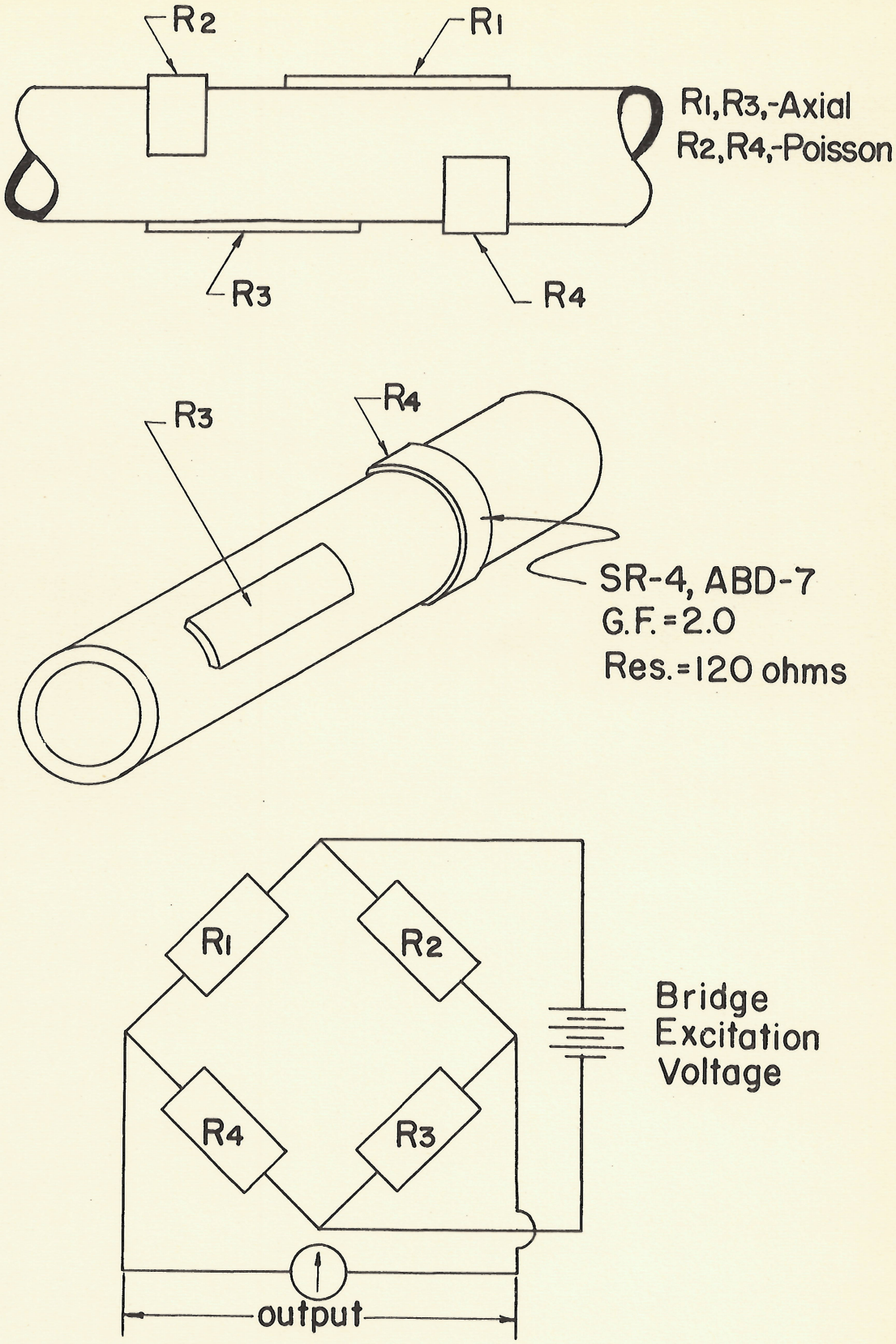

FIG. 6-Detail of Strain Gage Arrangement On Straight Section of Test Specimen

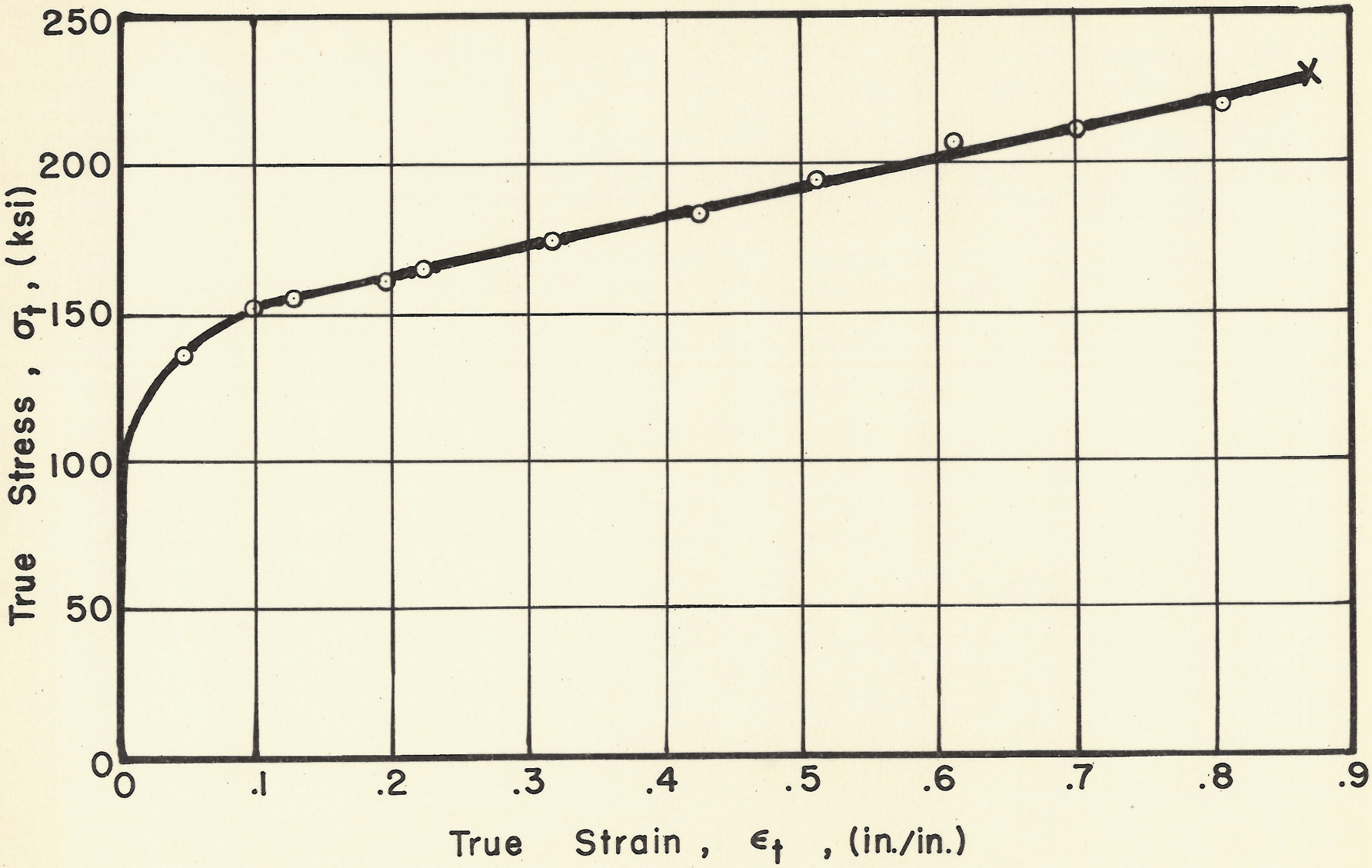

FIG. 7 – TRUE STRESS – STRAIN CURVE

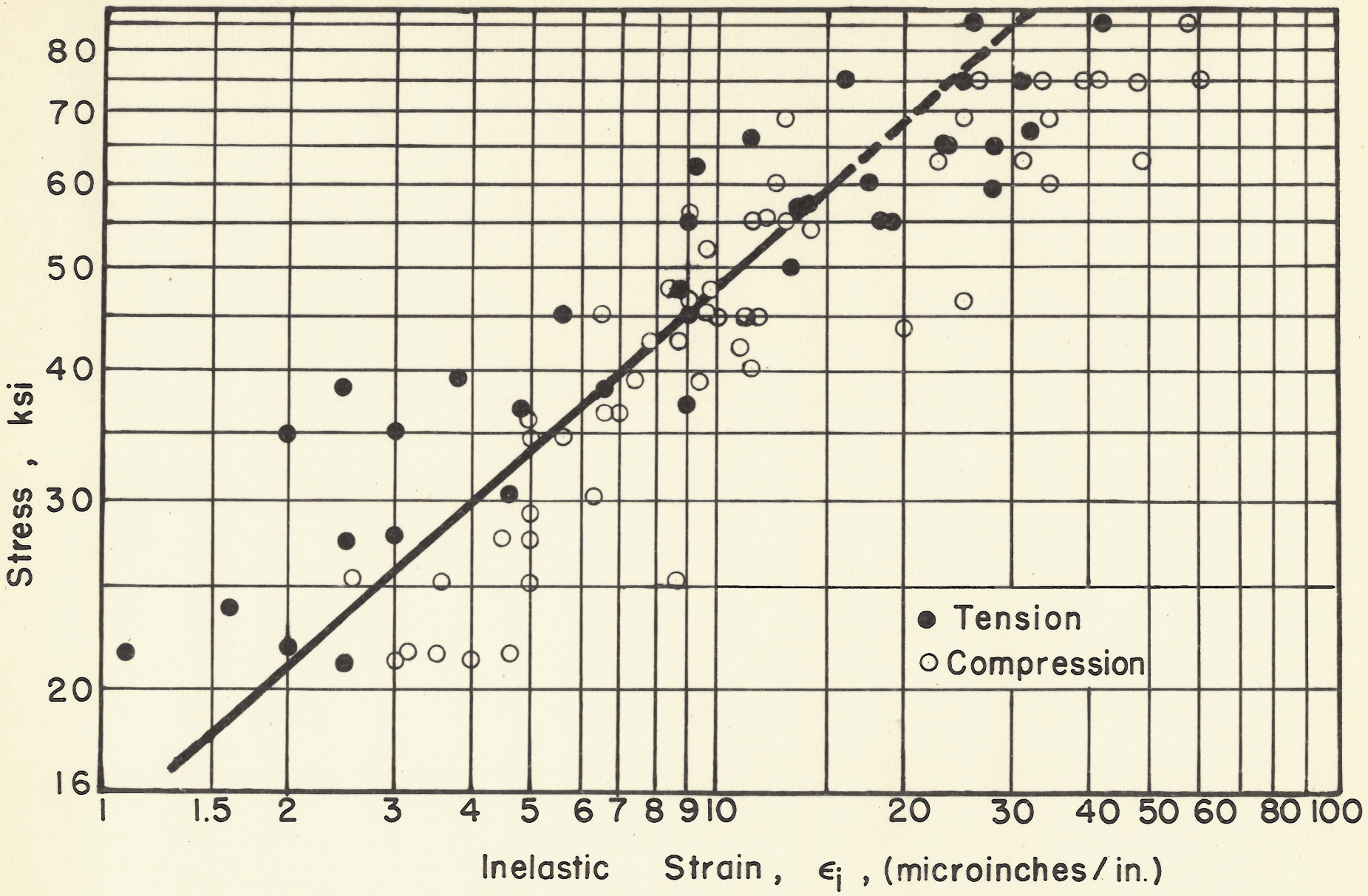

FIG. 8 – CYCLIC STRESS – INELASTIC STRAIN RESULTS

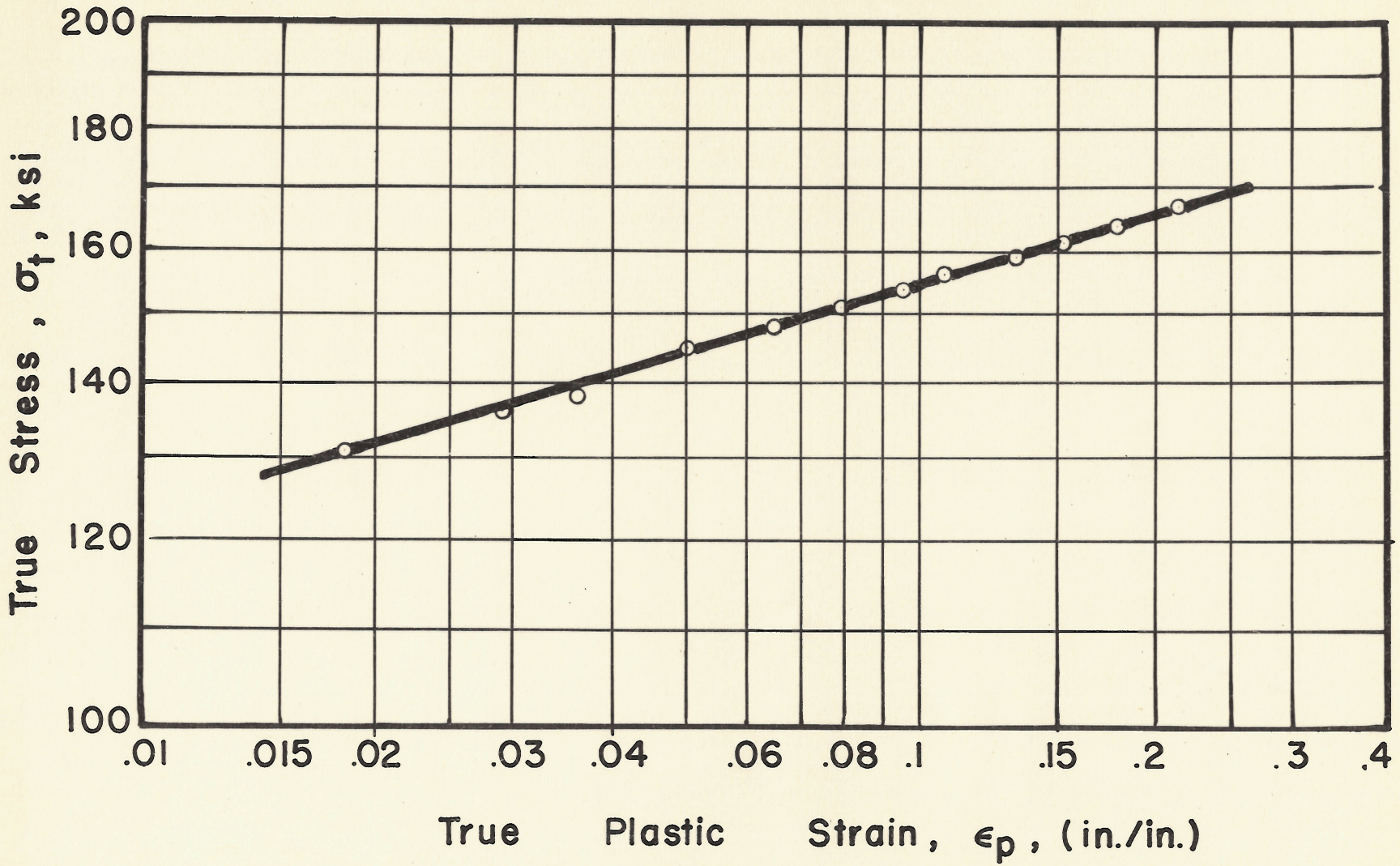

FIG. 9 – LOGARITHMIC STRESS – PLASTIC STRAIN CURVE

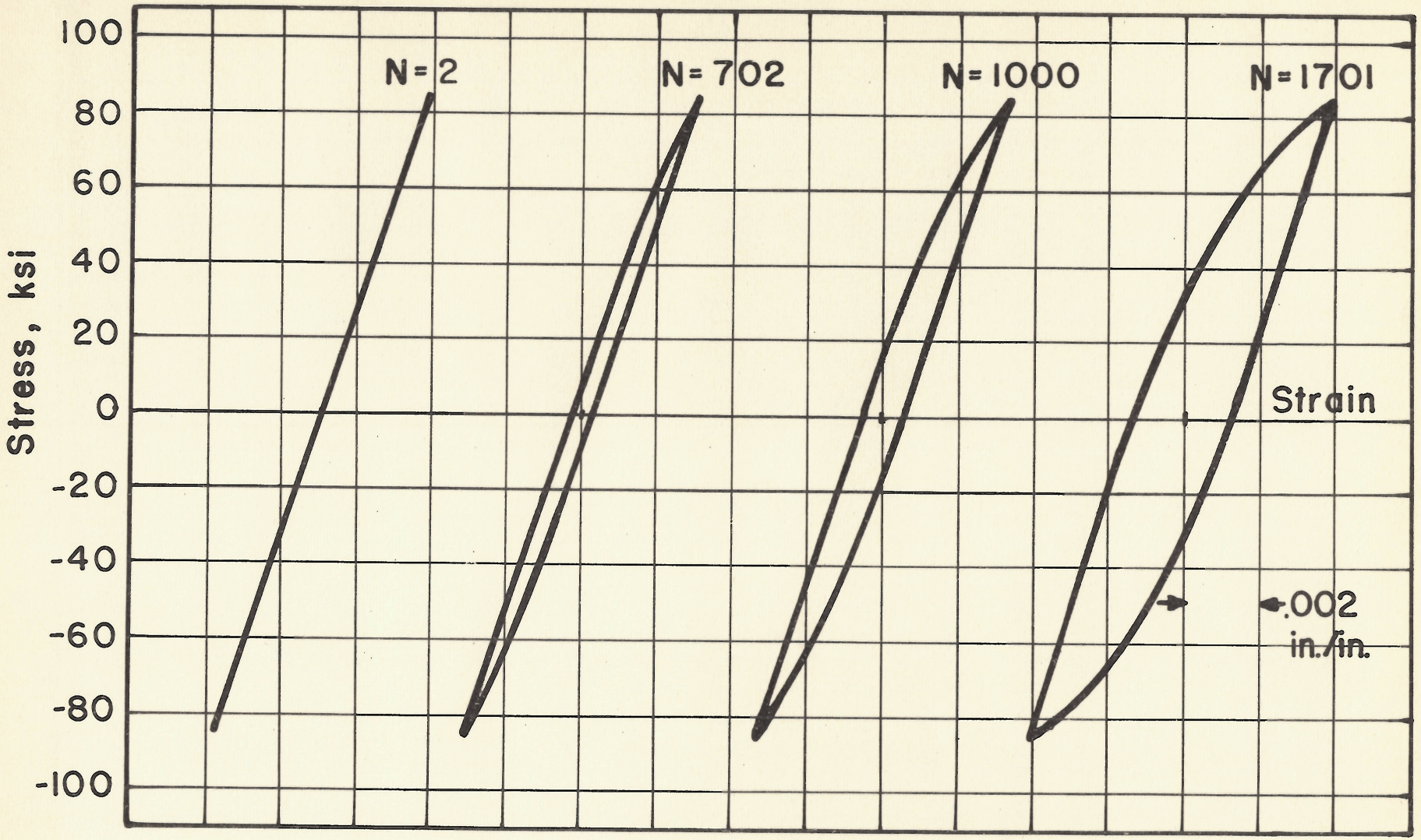

FIG. 10 - SAMPLE OF STRESS - STRAIN BEHAVIOR FOR LARGE STRESS AMPLITUDE (SPEC. NO. 10)

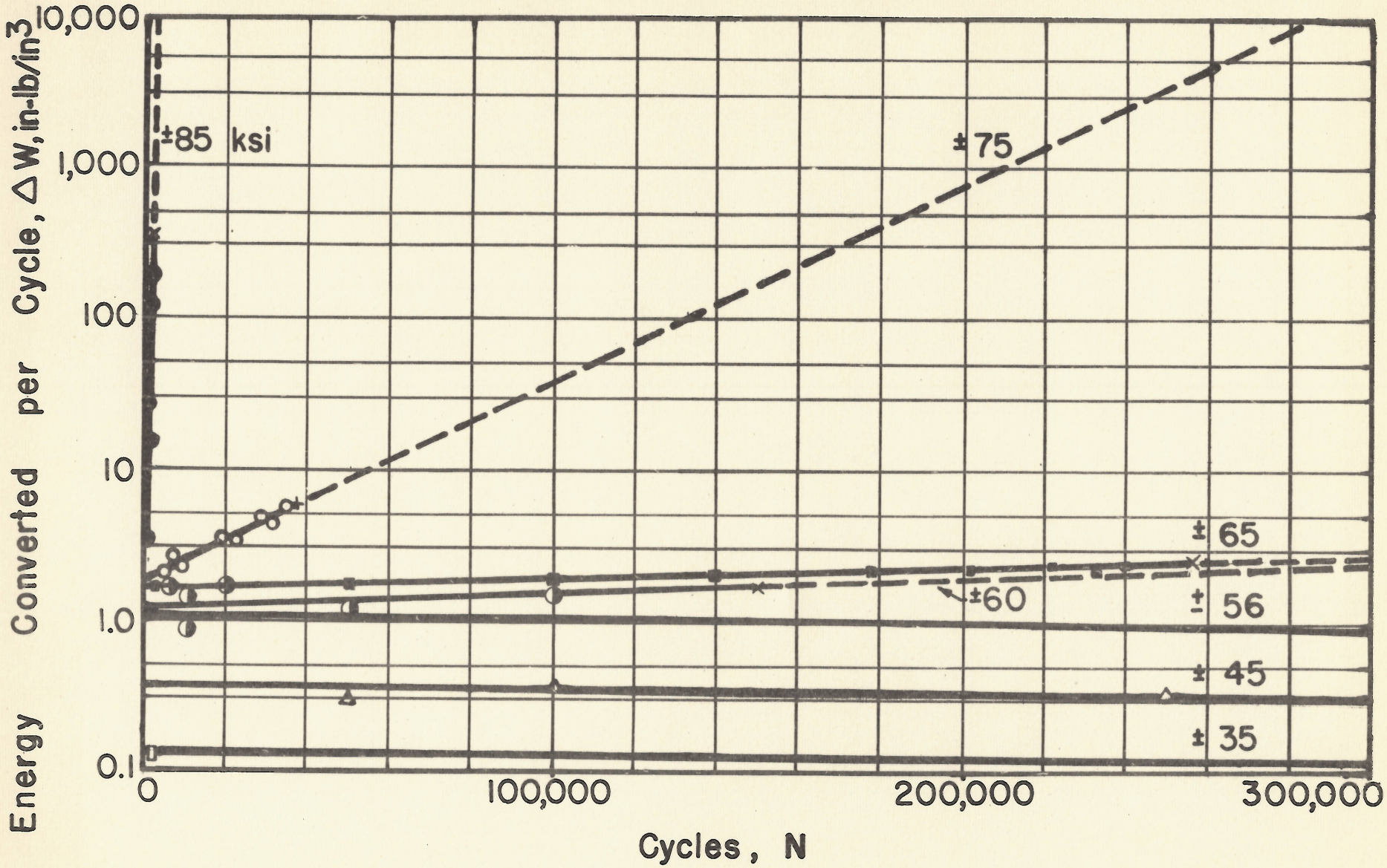

FIG. 11 - VARIATION OF HYSTERESIS ENERGY WITH CYCLES

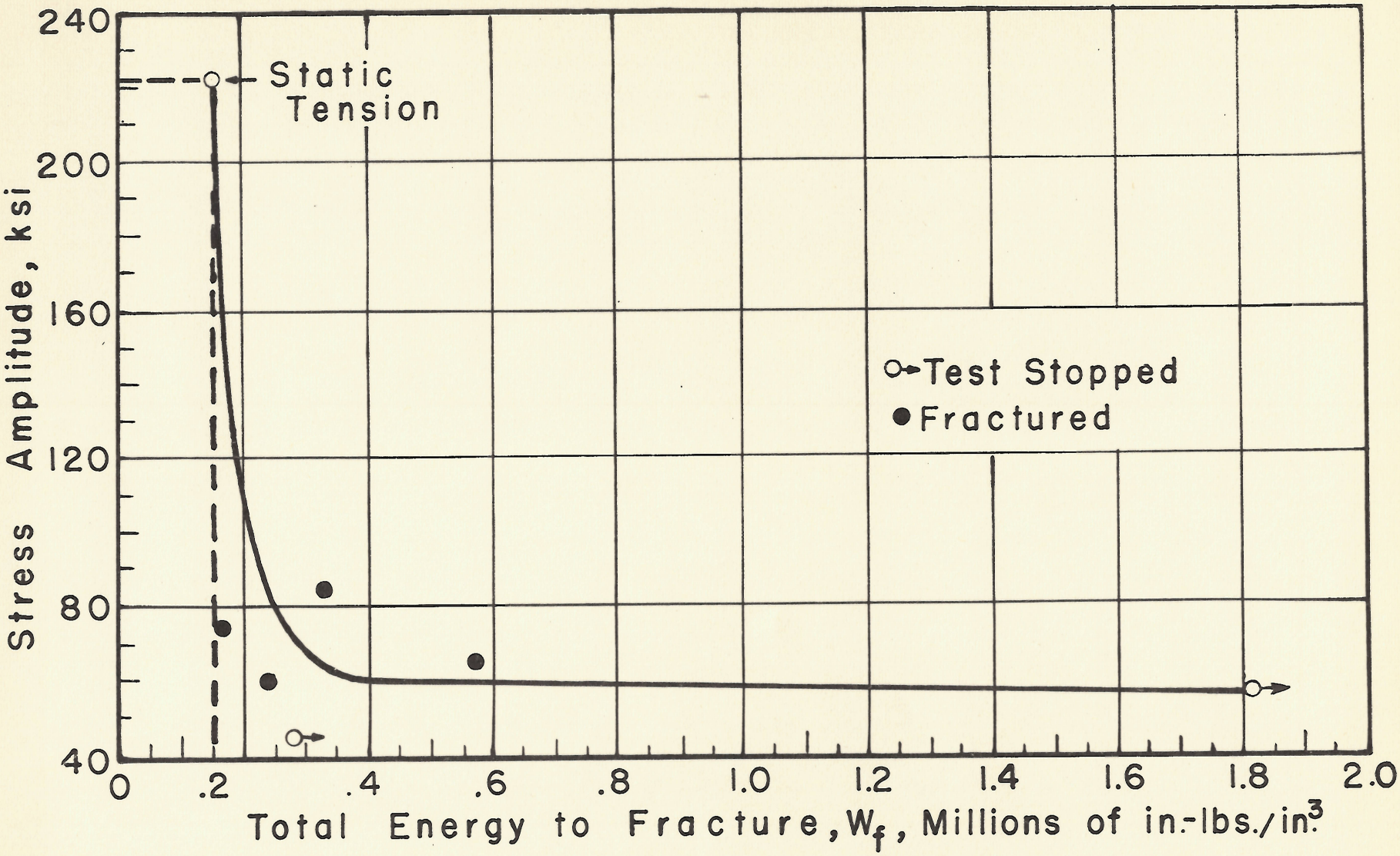

FIG. 12- RELATION BETWEEN STRESS AMPLITUDE AND TOTAL ENERGY TO FRACTURE

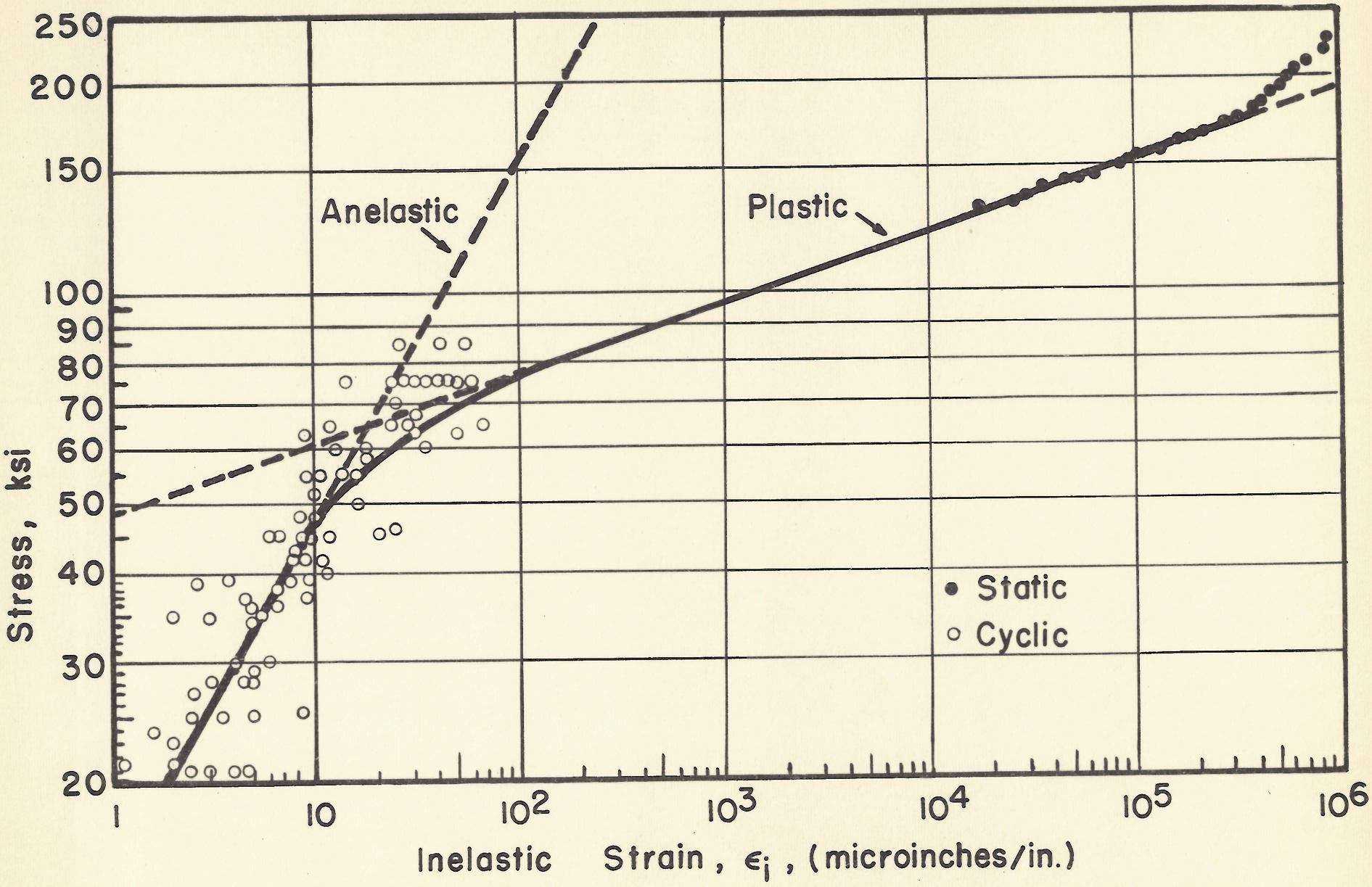

FIG. 13 – VARIATION OF INELASTIC STRAIN WITH STRESS

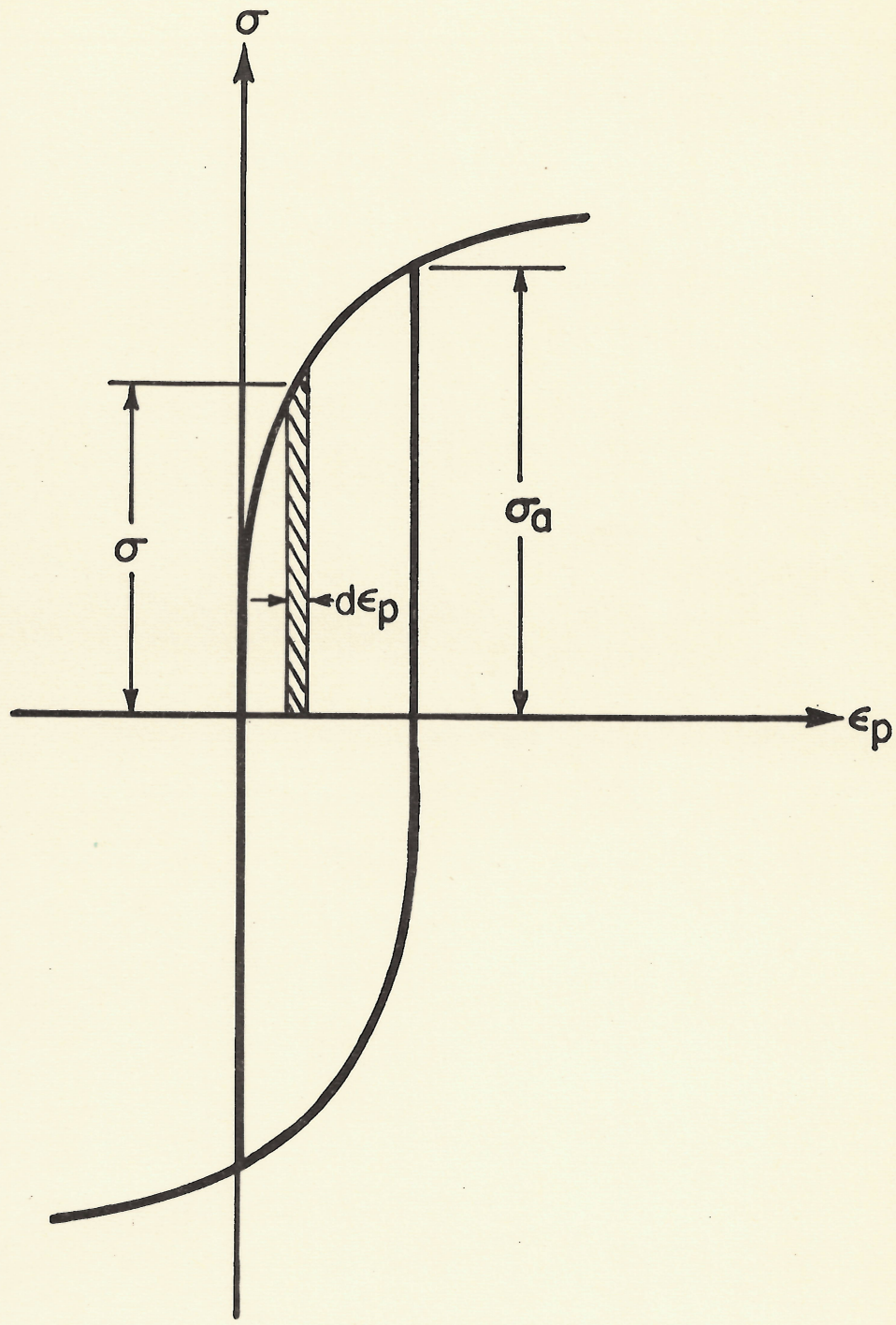

FIG. 14- MODEL OF $\sigma - \epsilon_p$ HYSTERESIS LOOP

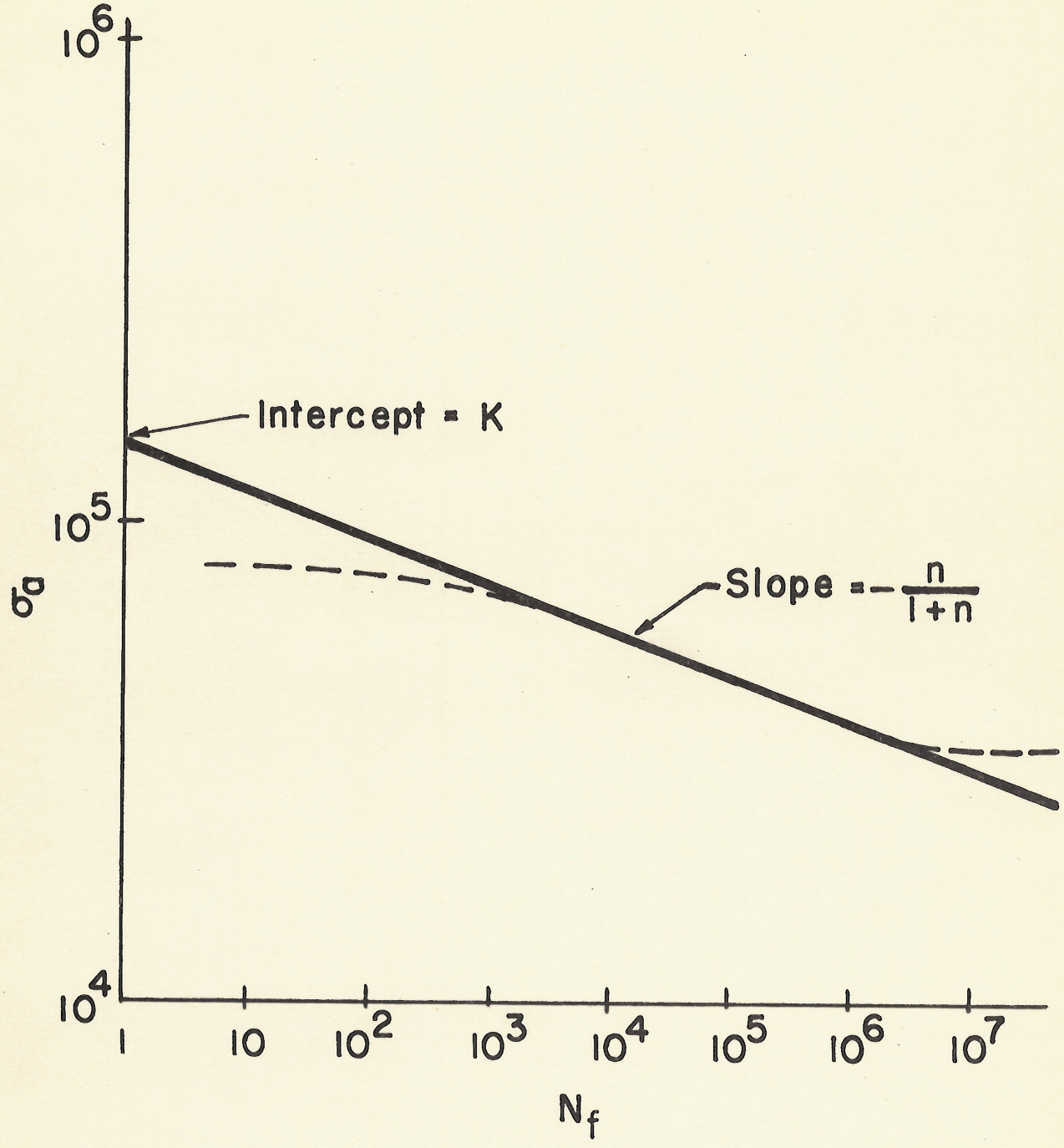

FIG. 15 – S - N CURVE OBTAINED USING ENERGY AS A CRITERION FOR FATIGUE

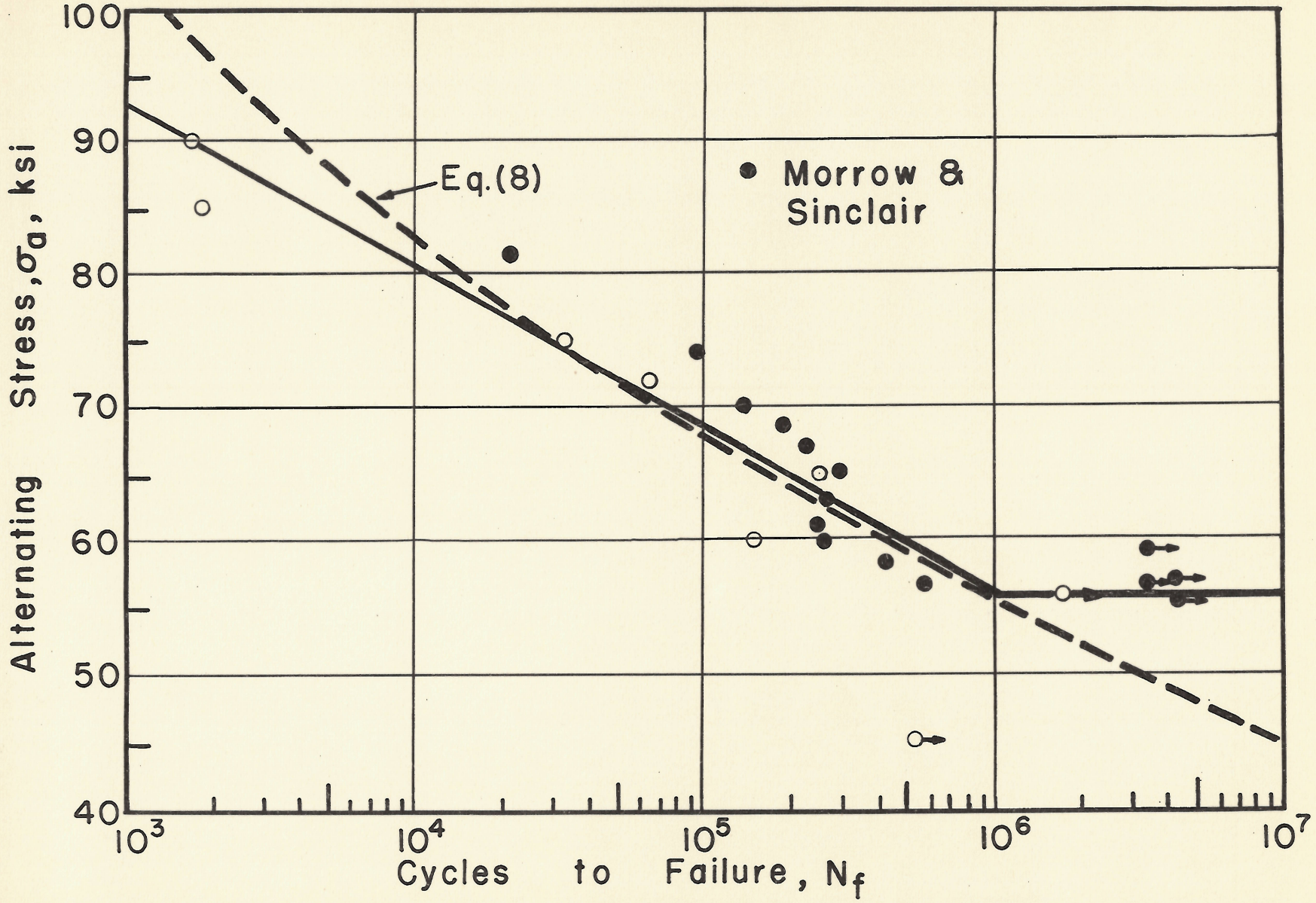

FIG. 16 COMPARISON OF TEST RESULTS WITH ANALYSIS